

Mechanistic Pathways for Ketene Dimerization

Karl Jug

Theoretische Chemie, Technische Universität Hannover

James Chickos

Department of Chemistry, University of Missouri at St. Louis, USA

Received June 30, 1975

A semiempirical MO method was used to calculate potential energy surfaces for ketene dimerization. One supra-supra and two supra-antara pathways were investigated. Six parameters were used to characterize the relative motion of individual groups. Two levels of approximation for the motion were considered. First, synchronous reaction pathways were followed, and a set of single-dimensional potential curves generated. Then, deviations from these synchronous reaction pathways were considered for each parameter and five two-dimensional potential surfaces for each pathway generated. Agreement with the available experimental data is satisfactory. However, we conclude that contrary to the Woodward-Hoffmann rules [1] the supra-supra pathway is allowed and the supra-antara pathways essentially forbidden. In the former case the local symmetry of the orbitals involved in the ring formation is not conserved during the reaction, in the latter case the nuclear repulsion is dominating.

Key word: Ketene dimerization

1. Introduction

Recently, interest in quantum chemistry has focused on the generation of potential energy surfaces for chemical reactions. The experimental data usually available include the potential energy of reactants and products, activation energy and equilibrium geometries of the molecules involved. From these points the theoretician is asked to determine properties of the intermediate states, including geometry and potential energy manifolds of reactant and product which are often difficult or impossible to investigate experimentally. To achieve this end, a variety of computation methods have been developed. With the presently available computers, semiempirical molecular orbital calculations of reactions of small organic systems are within reach.

We have chosen to investigate the dimerization of ketene for the following reasons: 1) The ground state geometries of ketene and diketene, both highly reactive molecules, have been determined [2, 3]; 2) the potential energy difference between the two compounds [4, 5] and the activation energy for the dimerization process in acetone have been measured [6e]; 3) the mechanism of the dimerization of ketene has not thoroughly been investigated on either an experimental or theoretical basis despite the commercial importance of both substances [6]; 4) the regiospecific head to tail dimerization of ketene is anomalous in comparison to the

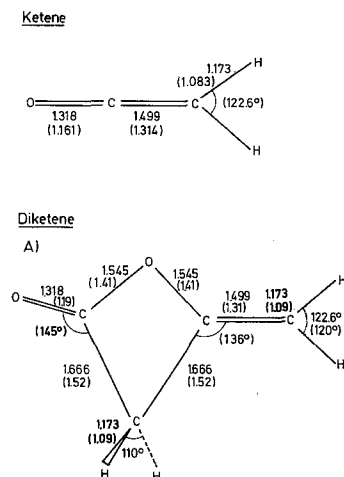


Fig. 1. Bond optimized lengths and bond angles in ketene and diketene. Experimental data in parentheses

1,3-diones that are produced in the dimerization of other ketoketenes [6a-c] and 5) the dimerization of ketene furnishes an interesting test case for the Woodward-Hoffmann rules for [2+2]cycloaddition reactions.

2. Method

We have employed a semiempirical MO method previously developed by Jug [7] and implemented by Coffey and Jug [8]. The scheme used was a modified INDO procedure in which the parameter formulas were developed on a symmetrically orthogonalized basis [9]. Different from Pople and collaborators [10], the following form of the resonance integral was introduced

$$H_{ab} = S_{ab}/2 \left[\frac{K_A - K_B}{2} (H_{aa} + H_{bb}) + \frac{1}{1 - S_{AB}^2} \frac{\rho_B - \rho_A}{\rho_B + \rho_A} (H_{aa} - H_{bb}) \right] + \frac{1}{R} \frac{d S_{ab}}{d R}$$

where ρ_A , ρ_B are modified Schomaker-Stevenson single bond covalent radii [11], S are overlap integrals and K adjustable atomic parameters to fit diatomic binding energies. The third term is the Linderberg term [12], the second a polarization term, the first term a correction term for truncation of the pertinent commutator equation [7].

This method is particularly apt to describe energy differences between reactants and products.

3. Energy Surfaces and Contour Diagrams

We first optimized the bond lengths of ketene and diketene starting with the experimental data of Bregman and Bauer [2] and Sheridan [3]. To reduce the computational complication of the subsequent energy surface calculations, we used the experimental bond angles and kept the ratio of $r_{C=O}/r_{C=C}$ constant and equal to the experimental ratio. The results are shown in Fig. 1. As usual in semi-

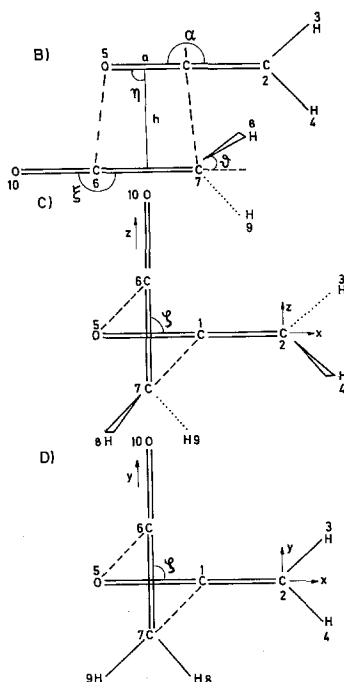


Fig. 2. One supra-supra pathway *B* and two supra-antara pathways *C* and *D* with various geometric parameters

empirical methods on this level the bond lengths are on the average 10% too long. The calculated dipole moments of 1.22 Debye for ketene and 4.07 Debye for diketene compare favorably with the experimental values of 1.41 Debye [13] and 3.5 Debye [14] respectively. The calculated dimerization energy

$$\Delta E_{\text{dim}} = E_{\text{diketene}} - 2E_{\text{ketene}}$$

makes diketene more stable by 36 kcal. In comparison the experimental heat of formation $\Delta H_f = -11.4$ kcal for ketene [4] and -45.47 kcal for diketene [5] yield a dimerization energy of about -23 kcal.

Three different approaches (Fig. 2) of the two ketene molecules to form diketene were studied. They are labelled *B*, *C*, *D* with the equilibrium geometry labelled *A*.

We chose to study these approaches because the unsymmetrical nature of ketene dimerization permits a discrimination between three physically distinct approaches of the two ketene molecules. These are shown in Fig. 2. The first approach describes the $[\text{C}^{\text{=O}}\pi 2_s + \text{C}^{\text{=C}}\pi 2_s]$ (*B*) and is forbidden by the Woodward-Hoffmann rules. The next two approaches can be described as $[\text{C}^{\text{=O}}\pi 2_s + \text{C}^{\text{=C}}\pi 2_a]$ (*C*), and $[\text{C}^{\text{=O}}\pi 2_a + \text{C}^{\text{=C}}\pi 2_s]$ (*D*); both are Woodward-Hoffmann allowed processes. The geometrical differences between approaches *B*, *C* and *D* should give rise to transition states of different energy, which could in principle be distinguished between by theoretical calculations. We chose pathways best described by a concerted

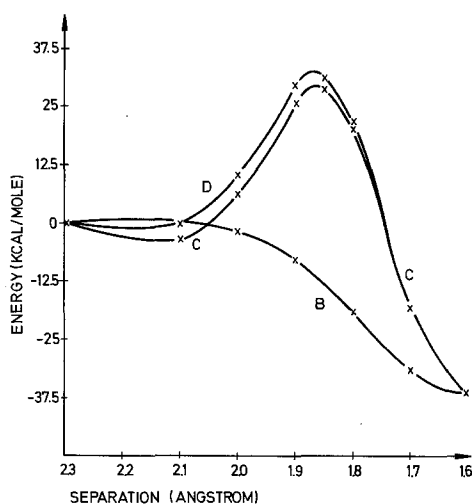


Fig. 3. Relative total energy (kcal) of diketene with respect to the separation h (Å)

reaction since diradicals seemed to be less likely as judged by experimental evidence obtained on similar reactions [15].

The following geometric parameter groups were used:

1. Intermolecular distance h between the midpoints of those C=O and C=C bonds of the ketenes which form the ring in diketene to characterize the separation between the reactants
2. Bond lengths a and c of the above mentioned C=O and C=C bonds to characterize stretching
3. Bond angle α for the vinyl group bending
4. Bond angle ζ for the carbonyl group bending
5. Angle set $\{\vartheta, \varphi\}$ for the methylene group bending and rotation about C(6)=C(7); angle ϑ is between C(7)–H(8) and the extension of C(6)=C(7), angle φ describes the rotation of the former bond about the latter; for *B*, φ is between the C(2)H(3)H(4) and C(6)C(7)H(8) planes
6. Angle sets $\{\zeta, \lambda\}$ and $\{\eta, \kappa\}$ describe the relative orientation of the two ketenes for cases *C* and *D*. The first set refers by angle ζ to the relative directions of the C(6)=C(7) and the C(1)=O(5) bonds and by angle λ to the rotation of the former bond about the latter. Similarly, the second set refers to the motion of the intermolecular distance about the C(1)=O(5) bond. Furthermore, the relation between the angles in each set is linear 1 : 1 relationship.

The CH bond lengths and the HCH angles were kept constant.

After test calculations we decided to use the intermolecular distance of 2.3 Å to represent infinity, since at smaller distances the effects of bonding between the two ketenes began to show.

First, we investigated a synchronous reaction behaviour for all three pathways *B*, *C*, *D*. Fig. 3 shows the potential curves obtained for ketene dimerization as a function of intermolecular distance h when parameter groups 2 to 6 were varied

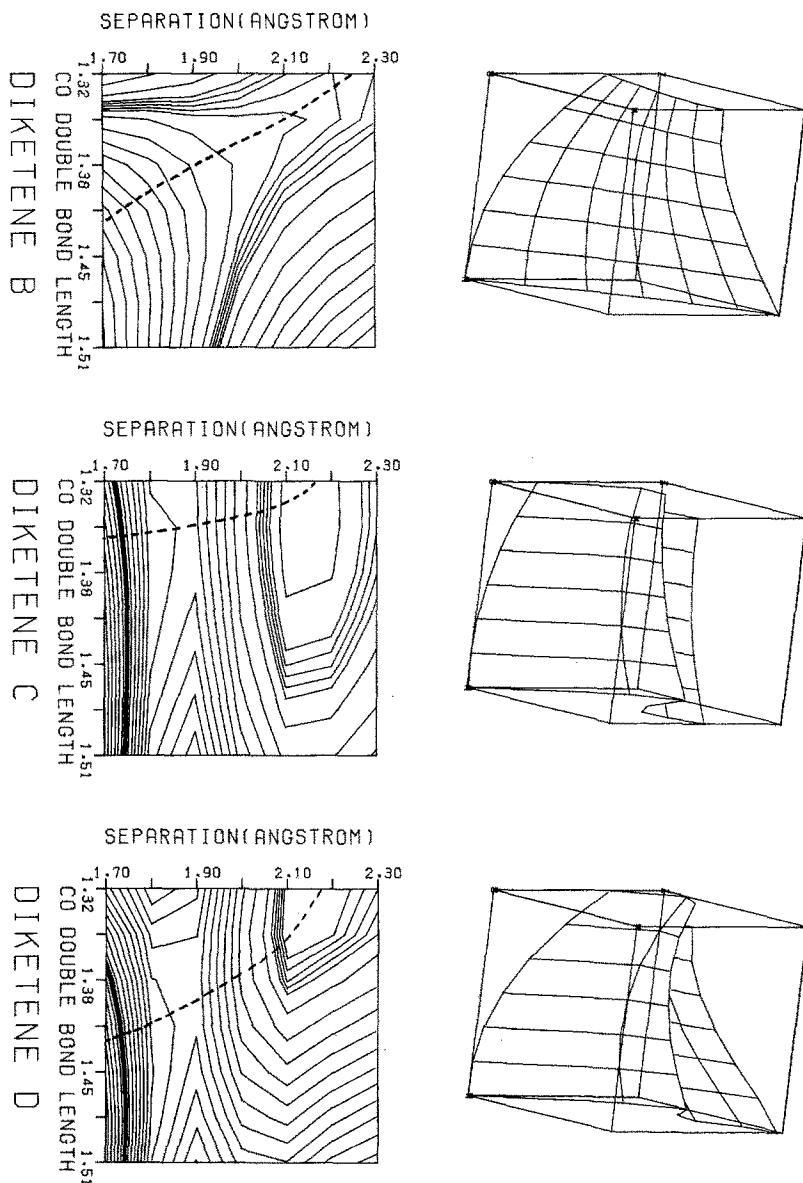


Fig. 4. Potential energy surfaces and contour diagrams for pathways *B*, *C* and *D* in dependence on double bond length a and separation h (Å). In these figures, two ketenes are represented approximately in upper left corner, diketene equilibrium by the lower right corner. Reaction pathway is represented by the dashed line

linearly with the intermolecular distance between 2.3 Å and 1.6 Å. An energy barrier of 33 kcal and 31 kcal/mole was obtained for the supra-antara pathways, *C* and *D*, but no barrier was detected for supra-supra pathway *B*.

To allow for a more detailed analysis, one of the parameters in the groups 2 to 6

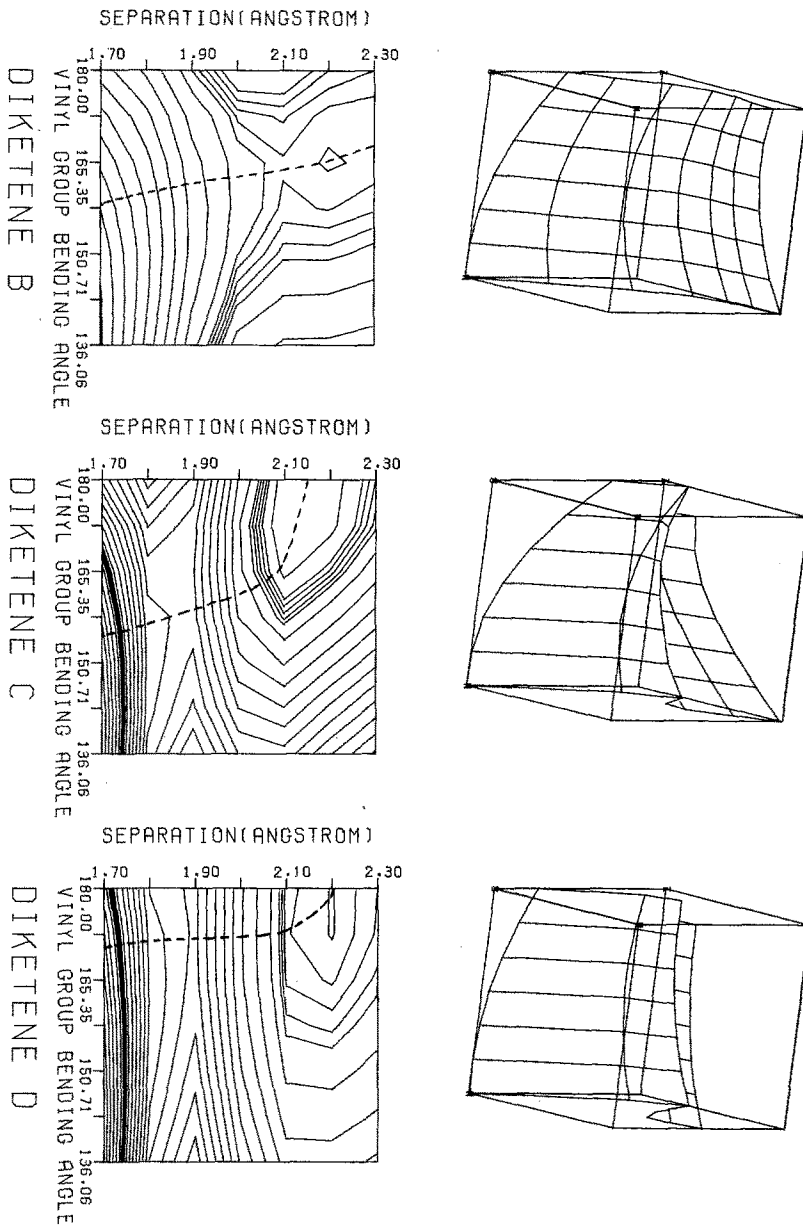


Fig. 5. Same as Fig. 4. Energy dependence on angle α of the vinyl group and separation

was allowed to vary freely while the rest were kept dependent on 1. That is the synchronous pathway of Fig. 3 was kept as a reference and deviations from synchronous behaviour for all pertinent geometric parameters were considered. The results are shown in Figs. 4-8. In these diagrams, the upper figures show the potential surfaces within a reference cube, the lower ones represent contour lines.

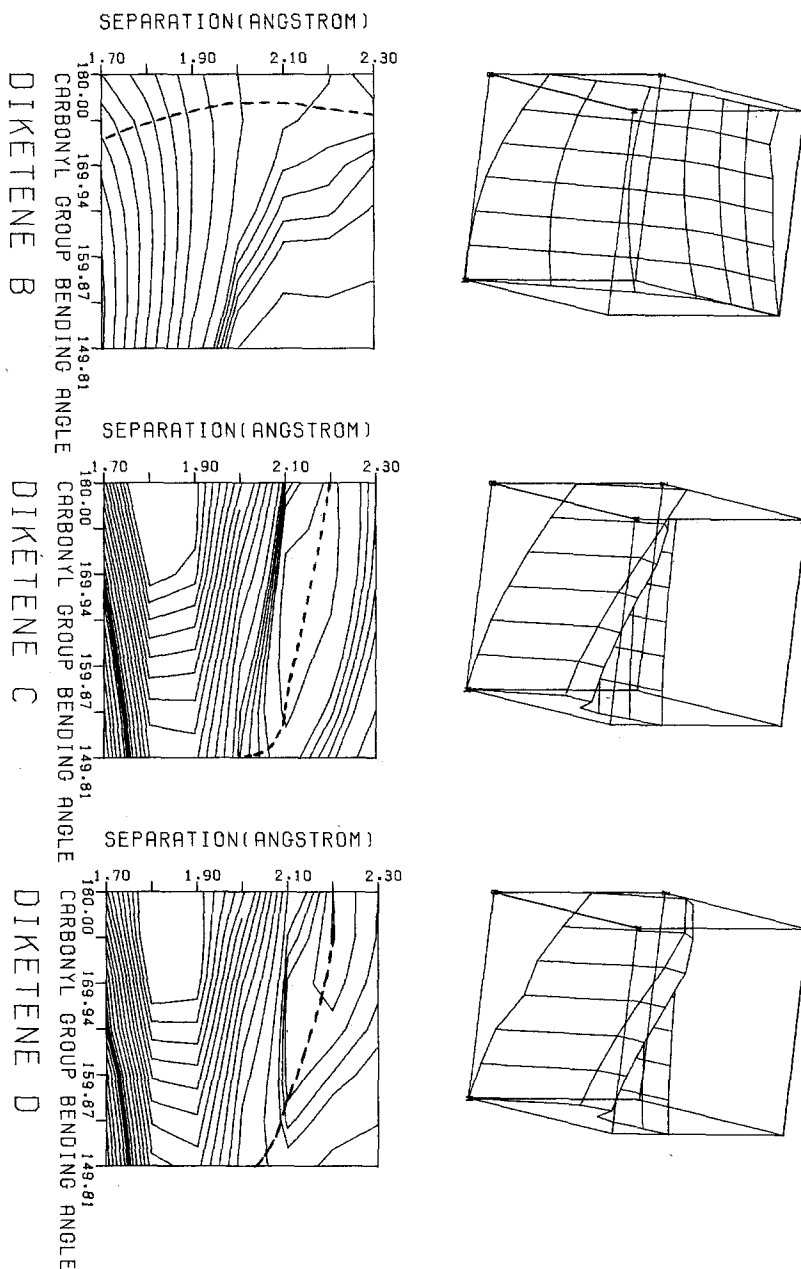


Fig. 6. Same as Fig. 4. Energy dependence on angle ξ of carbonyl group bending and separation

The energy difference is about 3 kcal for adjacent contour lines. For the flat part of the surface close to the separated ketenes a few more contours are introduced.

From Fig. 4 we conclude that for pathway *B* bond breaking of the double bonds parallels the closing in between the two ketenes with the former process

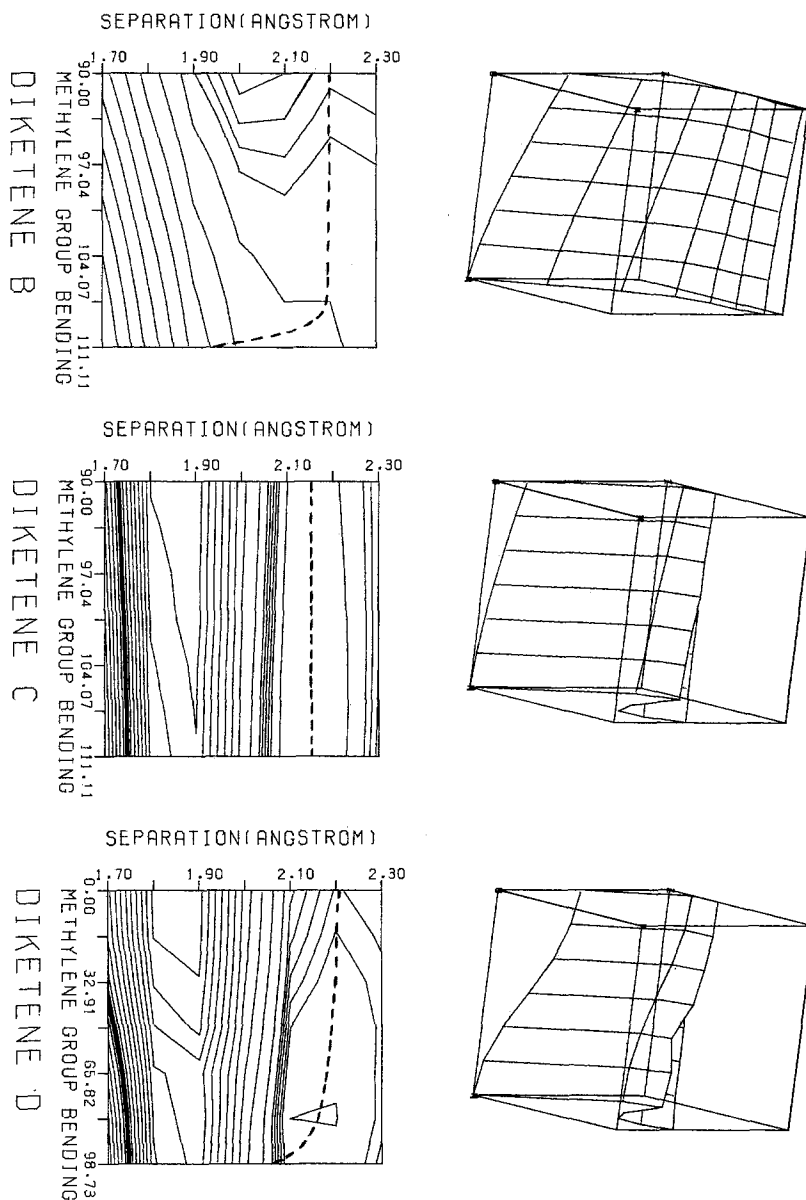


Fig. 7. Same as Fig. 4. Energy dependence on angle set $\{\theta, \varphi\}$ of methylene group bending and separation; φ coordinate is presented

being somewhat slower. For pathway *C* the character of the reacting double bonds in the ketene molecules is not perturbed until the two ketenes have reached the diketene equilibrium geometry. Pathway *D* suggests some bond breaking followed by complete bond formation before the final bond stretching occurs. *B* shows no barrier, the transition states of *C* and *D* have barriers of 22 kcal and 27 kcal with respect to two ketenes. We further conclude that in case *C* the molecules do not

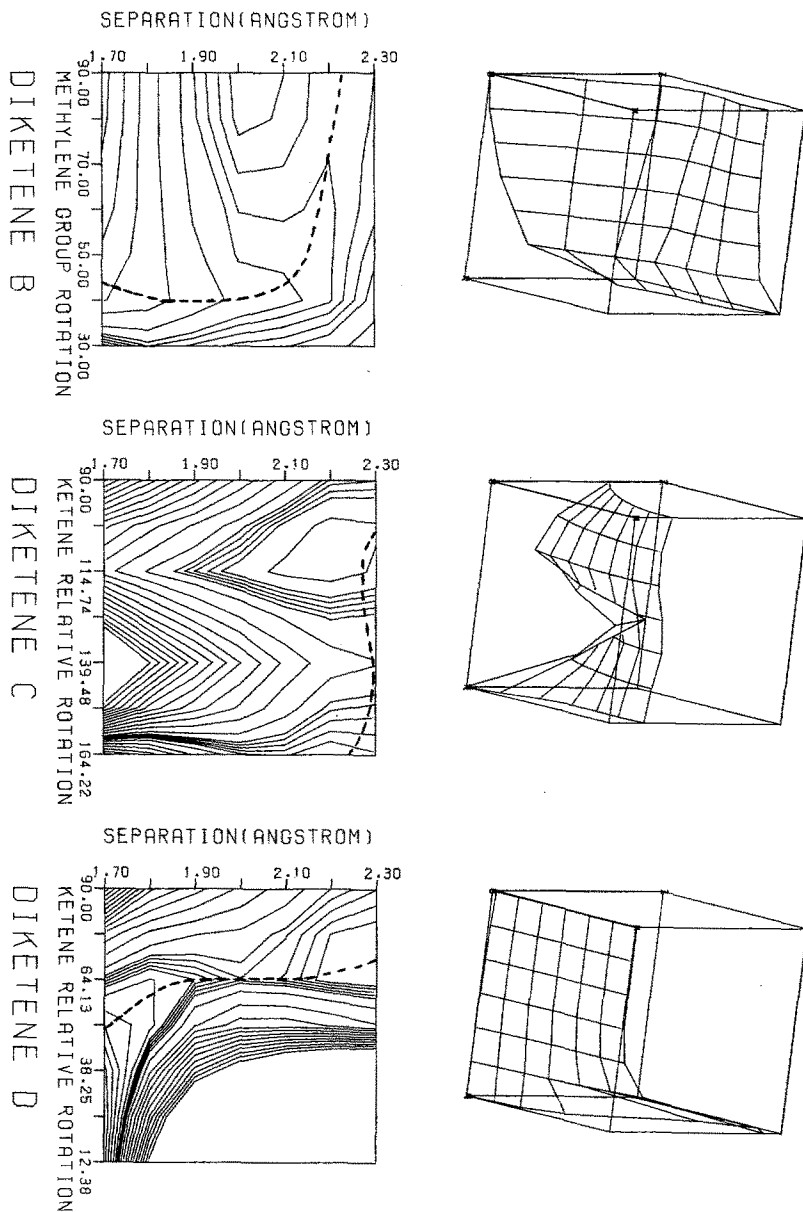


Fig. 8. Same as Fig. 4, except that in 8a diketene equilibrium is in the lower left corner. Energy dependence of B on angle ϕ of methylene group rotation and separation and on relative ketene orientations $\{\zeta, \lambda\}$ for C and $\{\eta, \kappa\}$ for D and separation; ζ and κ coordinates are presented

react until they are very close together and that the stretching vibration of ketene will not cause the reaction in pathways C and D .

From Fig. 5 it is apparent that for B the vinyl group bending is slower than the approach of the reactants. After some bending the vinyl group angle α stays almost constant between 170° – 160° before it finally bends to 129° . Cases C and D show a

Table 1. Sequence of rearrangements for pathways *B*, *C* and *D*

| <i>B</i> | <i>C</i> | <i>D</i> |
|-----------------------------|----------------------------|----------------------------|
| Bending of methylene group | Parallel orientation | Bending of methylene group |
| Rotation of methylene group | Bending of methylene group | Bending of carbonyl group |
| Breaking of double bonds | Bending of carbonyl group | Parallel orientation |
| Bending of vinyl group | Bending of vinyl group | Breaking of double bonds |
| Bending of carbonyl group | Breaking of double bonds | Bending of vinyl group |

similar pattern as in Fig. 4: very little bending or some bending before the equilibrium configuration of diketene is closely approached. Again *B* shows no barrier, whereas *C* and *D* have barriers of 22 kcal and 27 kcal, respectively.

Fig. 6 describes the behaviour of the carbonyl group bending as the reactants approach each other. Pathway *B* shows almost no bending before the two ketenes are very close. This is in agreement with the finding from Fig. 4 that the double bond character is only slowly changed during the reactants' approach. In cases *C* and *D*, however, complete bending of the carbonyl group angle ξ has to occur long before the reaction takes place in order to make the barrier height as favorable as possible. The barrier is 19 kcal in both cases. Fig. 7 suggests complete bending of the methylene group before reaction for all three pathways. No barrier is encountered in pathway *B*, but a height of 26 kcal and 25 kcal occurs in *C* and *D*.

Rotation of the methylene group about the adjacent C(6)=C(7) bond is depicted in Fig. 8 for pathway *B*. It can be explained as a superposition of two opposing trends: electronic attraction favors planar arrangement ($\varphi = 0^\circ$) which is opposed by nuclear repulsion. The former dominates for large separation of the reactants, the latter for the region of diketene formation. Maximum rotation is about 40° . The relative orientation of two ketenes is described by angles ζ and κ for cases *C* and *D*. Pathway *C* can lead to a reaction only along a coordinate which lets it coincide with pathway *B* already for large separations between the reactants. Any other approach will lead to an exceedingly high barrier. In case *D* a similar conclusion is reached. The two ketenes have to approach each other fairly closely before the "on top" position is given up in favor of the planar ring arrangement of *B*. During the approach of the two ketenes, the angle κ of rotation of the two ketenes stays close to 64° , whereas the ring forming C=O and C=C bonds are getting close to 1.8 Å separation. Since the angle set $\{\eta, \lambda\}$ is changing accordingly with *h* these two ketene bonds approach parallel orientation thus aiming at pathway *B*. The minimal barrier in case *D* is only 2 kcal. So we conclude that such a pathway is in principle possible.

The sequence of rearrangements is listed in Table 1. Further general observations are: In the case of "forbidden" reactions the reaction pathway is determined by the minimal height of an intermediate barrier. Consequentially a reaction coordinate does not necessarily follow the locally optimal pathway. This would often lead to a dead end in a reactant valley. The two valley structure of such pathways was already discovered for electrocyclic reactions by Dewar and Kirschner [16]. A gradient method would usually lead past the saddle point and is thus worthless unless it has certain restrictions built in. Such restrictions do not

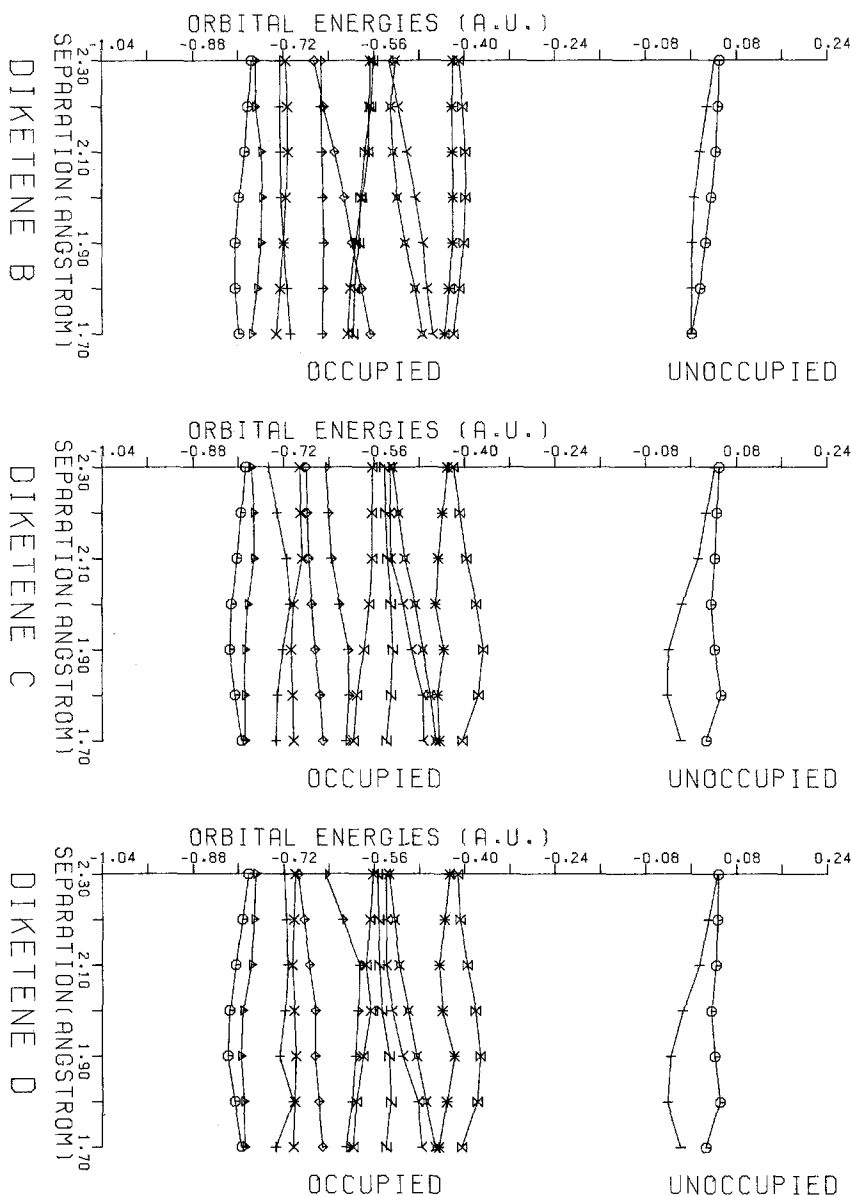


Fig. 9. Orbital energies related to Fig. 3 for pathways *B*, *C* and *D* in dependence of separation

seem to be more valuable than the assumption of some knowledge about the reaction such as the one used here.

4. Orbital Energies and Woodward-Hoffmann Rules

At this point, it might be interesting to discuss orbital plots which are frequently used as a verification of the Woodward-Hoffmann rules. The potential

energy curves of Fig. 3 show one allowed pathway of supra-supra type and two forbidden pathways of supra-antara type. The Woodward-Hoffmann rules in their simplest form would consider the C=O and C=C bond interactions of the two ketenes which form the ring. From these rules a concerted process should yield a forbidden supra-supra pathway and two allowed supra-antara pathways. Since this is in disagreement with our findings, this point should be investigated further. For this purpose we present the orbital diagrams based on calculations for Fig. 3 in Fig. 9. The highest occupied orbital of *B* has no significant maximum, whereas such a maximum is recognized in pathways *C* and *D*. The latter means that the lowest unoccupied orbital of the first ketene interacts strongly with the highest occupied orbital of the second ketene during the reaction. Lack of symmetry in the reacting system prevents crossing of the orbital energy levels. Thus the conclusion of Fig. 9 is in agreement with those of Fig. 3.

5. Conclusion

The dimerization of ketene according to these calculations appears to violate the Woodward-Hoffmann rules. The dimerization of ketene appears to best be described as a $[\pi 2_s + \pi 2_s]$ cycloaddition reaction and a small barrier to reaction is anticipated for this process on the basis of these results¹. Experimentally the rate of disappearance of ketene in acetone has been found to obey a bimolecular rate law and an activation energy of 11 kcal has been reported [6e].

It appears that the formation of diketene cannot be considered solely on the basis of nodal properties of localized double bonds alone. In particular, local symmetry of interacting MO's of ketene is not conserved during the reaction. The interaction of the various bonds, governed by both electronic factors as well as nuclear repulsion, is most important in this reaction. A recent investigation of ethylene dimerization [17] showed already the importance of nuclear repulsion. Also examples that frontier orbitals do not always dominate the reaction have been reported [18, 19].

Acknowledgement. The calculations were made possible by a generous allotment of computer time by the University of Missouri at St. Louis.

References

1. Woodward, R.B., Hoffmann, R.: *The Conservation of Orbital Symmetry*. Weinheim: Verlag Chemie 1971
2. Bregman, J., Bauer, S.H.: *J. Am. Chem. Soc.* **77**, 1955 (1955)
3. Sheridan, J.: *Advan. Mol. Spectry. (Proc. 4th Intern. Meeting Mol. Spectry.)* Pergamon Press, London, 1962, p. 139 and cited in: *Technique of organic chemistry*, Vol. IX (2nd Ed.) Part II, p. 700, W. West., Ed. New York: Interscience Publishers 1970
4. Nuttall, R.L., Laufer, A.H., Kilday, M.V.: *J. Chem. Thermodyn.* **3**, 167 (1971)
5. Mansson, M., Nakase, Y., Sunner, S.: *Acta Chem. Scand.* **22**, 171 (1968)
6. (a) Hanford, W.E., Sauer, J.C., in: *Organic reactions*, Vol. 3, pp. 108-140, R. Adams *et al.*, Eds. New York: Wiley 1946
(b) Lacey, R.N., in: *The Chemistry of alkenes*, S. Patai, Ed., pp. 1182-1197. New York: Interscience Publishers 1964

¹ On the CI level, a barrier of 6 kcal at 2.1 Å is indeed found for pathway *B*. CI does not change any of the other results significantly.

- (c) Ulrich, H.: Cycloaddition reactions of heterocumulenes, Vol. 9, Chapt. 2. New York: Academic Press 1967
- (d) Rice, F.O., Roberts, R.: J. Am. Chem. Soc. **65**, 1677 (1943)
- (e) Rice, F.O., Greenberg, J.: J. Am. Chem. Soc. **56**, 2132 (1934)
7. Jug, K.: Theoret. Chim. Acta (Berl.) **30**, 231 (1973)
8. Coffey, P., Jug, K.: J. Am. Chem. Soc. **95**, 7575 (1973)
9. Löwdin, P.O.: J. Chem. Phys. **18**, 365 (1955)
10. Pople, J.A., Beveridge, D.L., Dobosh, P.A.: J. Chem. Phys. **47**, 2026 (1967)
11. Schomaker, V., Stevenson, D.P.: J. Am. Chem. Soc. **63**, 37 (1941)
12. Linderberg, J.: Chem. Phys. Letters **1**, 39 (1967)
13. Johnson, H.R., Strandberg, M.W.P.: J. Chem. Phys. **20**, 687 (1952)
14. Roberts, J.D.: J. Am. Chem. Soc. **71**, 843 (1949)
15. Rey, M., Roberts, S., Dieffenbacher, A., Dreiding, A.S.: Helv. Chim. Acta **53**, 417 (1970); Brady, W.T., Roe, R.Jr.: J. Am. Chem. Soc. **92**, 4618 (1970)
16. Dewar, M.J.S., Kirschner, S.: J. Am. Chem. Soc. **93**, 4291 (1971)
17. Coffey, P., Jug, K.: Theoret. Chim. Acta (Berl.) **34**, 213 (1974)
18. Devaquet, A.J.P., Hehre, W.J.: J. Am. Chem. Soc. **96**, 3644 (1974)
19. Berson, J.A., Salem, L.: J. Am. Chem. Soc. **94**, 8917 (1972); Berson, J.A.: Accounts Chem. Res. **5**, 406 (1972)

Prof. Dr. K. Jug
Theoretische Chemie
TU Hannover
D-3000 Hannover 1
Callinstr. 46
Federal Republic of Germany